Electronic excitations in nanoscale systems with helical symmetry

1994 J. Phys.: Condens. Matter 6 3697

(http://iopscience.iop.org/0953-8984/6/20/009)

J. Phys.: Condens. Matter 6 (1994) 3697–3706. Printed in the UK

Electronic excitations in nanoscale systems with helical symmetry

P J Lin-Chung and A K Rajagopal
Naval Research Laboratory, Washington, DC 20375, USA

Received 30 November 1993, in final form 7 March 1994

Abstract. A complete set of helically symmetric wave functions is constructed and is used to set up the Bloch-like states for describing the electronic band structure of nanoscale systems with helical symmetry. Various helical arrangements leading to different graphitic tubules may be obtained by rolling the two-dimensional honeycomb lattice into a cylinder subjected to appropriate periodic boundary conditions. A discussion of the symmetries of these helices is given. This method is applied to study the electronic structure of graphitic tubules and is compared with other methods found in the literature.

The discovery of fullerene tubules [1, 2] has opened up new possibilities of light-weight, high-strength materials with interesting mechanical and electrical properties. In order to gain insight into the properties of such tubules, two theoretical models have been proposed in the literature. In one, the electrons of the system are thought to be mutually interacting while moving on the surface of a cylinder much like the free electron model of the interacting electrons in a solid. In the other model, the electrons belong to a graphite sheet of carbon atoms rolled into a cylindrical tube of constant radius. These models have served different purposes. The first approach admits of theoretical analysis of the many-electron interactions, and interesting mesh-like energy structures for their plasma modes and Kohn anomalies are obtained [3–5]. In [4] magnetoplasma oscillations were also studied. The second approach has been used to determine the physical properties reflecting the various possible geometric structures associated with the atomic disposition in helical motifs of varied types [6–8]. White *et al* [8] have given an extensive summary of the work on fullerenes including the tubule structures. They found the helical and rotational symmetries of the honeycomb lattice of carbon atoms wrapped on a cylinder necessarily lead to a variety of helical motifs important in determining the metallic (serpentine) and semiconducting (saw-tooth) properties of these tubules; these are missed in the electron gas model.

The purpose of this paper is to offer an alternative model of interacting electrons on a cylinder but now starting from the helix. It is described in terms of helical-symmetry-adopted states characterized by two parameters of the helix, the pitch and the pitch angle. We first construct a complete set of wave functions that have the correct helical symmetry of the empty lattices associated with different helical arrangements of the atoms. We have incorporated this into a two-dimensional electron gas model [9] to exhibit the modifications due to lower helical symmetry on the plasma properties of the higher-cylindrical-symmetry electron gas model quoted above. We have also investigated the effects of a constant magnetic fields along the tube axis. In the present work, we proceed to construct Bloch functions associated with the graphitic tubules and study the single-particle band structure properties of such systems. We relate the results obtained to those found by other authors

using different techniques (using tight-binding methods [6–8, 10, 11]; using the $k \cdot p$ method [12]; [12] also contains an examination of the magnetic field effects; and using the *ab initio* molecular dynamics technique [13]).

Just as the classification of plane wave states of the interacting electron gas in the empty lattice gives powerful insight into the electronic structure of the solid state system, the complete set of helical wave states can lead to useful insight into the electronic states of the helical arrangements of atoms on a cylinder by means of a suitable mathematical transformation of the complete set of cylindrical wave functions. Since the helical system has a lower symmetry than a cylindrical system, the mathematical transformation introduced here is non-trivial. It is applicable both to systems with additional rotational symmetry such as graphitic tubules and also to systems without any rotation symmetry such as helical polymer chains (see, for example, [14]). The former systems have their pitch commensurate with the periodicity along the tubule axis, whereas the latter do not.

We first observe that helical wave states are parametrized by the pitch angle, β, and the pitch p, of the spiral. These parameters are related to the arrangement of the periodic graphitic motif on the tubule by simple relations, which are derived in this paper. We may also point out that the helical-symmetry-adopted approach advocated here for elucidating the electronic structure of the helical motifs of atoms arranged on a cylinder is much like the plane wave basis states in describing the electronic structure of crystalline solids. Instead of the usual tight-binding method with plane waves, we suggest employing helical waves. Many-electron theory based on helical waves [9] in place of the cylindrical waves reflects the salient features of the helical structures even if we do not include the actual atomic structure, much as the *empty lattice* construction exhibits the crystal symmetry properties of the solid. With these considerations in view, we present here a theory of the electronic states of helical tubules based on helical waves.

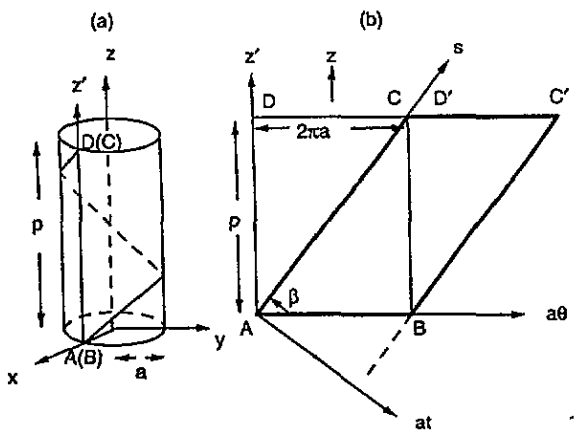

Figure 1. (a) The geometry of an isolated helix with pitch p and radius a. (b) The rectangle ABCD and the parallelogram ABC′D′ are obtained by unrolling the cylindrical surface after a cut is made along line AD and along the spiral path, respectively. The cylindrical surface coordinate system $[z', a\theta]$, and the new helical coordinate system (s, at) are shown. p and β are the pitch and pitch angle of the spiral, respectively.

We first consider one pitch of a single uniform helix. The geometry of the helix with pitch p, wound on a right circular cylinder of radius a, shown in figure 1, is characterized

by any arbitrary translation, h, along the axis of the cylinder accompanied by a concomitant rotation, $\varphi(h) = 2\pi h/p$, about the axis. The pitch angle, β, of the helix is defined as $\tan\beta = p/2\pi a$, with $0 < \beta \leqslant \pi/2$.

As described in figure 1, unwrapping the cylinder in two ways, one along the vertical line AD on the cylinder, leading to a rectangle ABCD in figure 1(b), and one along the helical path, leading to the parallelogram ABC'D', clearly exhibits basic features of the helix. Note that in figure 1(a), z and z' represent the axis of the cylinder and an axis parallel to it on the surface of the cylinder, respectively. The lines AD and BC are $[z', \theta = 0]$ and $[z', \theta = 2\pi]$, respectively.

When the cylinder is cut along AD and spread into a plane as in figure 1(b), the helix A(B)D(C) in figure 1(a) becomes the diagonal AC of the rectangle whose base AB is the circumference of the base circle of the cylinder. The cylindrical coordinate system becomes the two-dimensional $[z', a\theta]$ rectangular coordinate system of figure 1(b). In the study of the electronic structures of graphite tubules using a tight-binding method, many authors have chosen such a coordinate system [10, 11].

When the cylinder in figure 1(a) is cut along the helix and spread into a plane, the parallelogram ABC'D' is formed. AD' and BC' are in fact the identical cut edges associated with the helix and will coincide when ABC'D' is rolled back about the z-axis to reform the cylinder of figure 1(a). A rotation through 2π brings points B, D' back to points A, D and brings C' to C, and the line BC' coincides with AC, forming the helix. In the planar surface picture, we choose to employ a new rectangular helical coordinate system, (s, at), as shown in figure 1(b). The s-axis is along the helical line AC, and the at-axis is perpendicular to the s-axis. The (s, at) are related to the $[z', a\theta]$ by the following equations:

$$s = z'\sin\beta + a\theta\cos\beta \qquad at = -z'\cos\beta + a\theta\sin\beta. \tag{1}$$

The ranges $s : (-\infty, \infty)$, $t : (0, 2\pi\sin\beta)$ correspond to $z' : (-\infty, \infty)$, $\theta : (0, 2\pi)$.

We observe that the basic properties of the helix can be visualized from the parallelogram ABC'D' using the (s, at) coordinate system. This has the advantage over the $[z', a\theta]$ system when more complicated helical motifs are considered. A cylinder with several non-equivalent helices of the same pitch and pitch angle is obtained by starting each helix from a point on the base circle and running up the helical path in the same way as the single helix was described above. The seed points on the base circle may or may not possess a rotational symmetry among them. These helices then appear as parallel lines inside the rectangle and the parallelogram in figure 1(b) and these lines need not be equally spaced if there is no rotational symmetry to start with.

The consequences of these properties are now explored in detail.

(i) Each line represented by $t = t_0$ in the (s, at) system maps back to the surface of the cylinder as a helix passing through the point $[z' = 0, a\theta = at_0/\sin\beta]$. Thus the line AC ($t = 0$) corresponds to the helix passing through [0, 0]. This follows from equation (1). The generator of the translation along the helix may then be represented by the operator P_s in the (s, at) system of by $P + (2\pi/p)L$ in the $[z', a\theta]$ system, P being the generator of the translations parallel to z, and L the generator of a rotation around the z-axis,

$$P + (2\pi/p)L = (\sin\beta)^{-1}P_s. \tag{2}$$

(ii) Because the segment BC' rolls back to the AC, a fundamental requirement on the wave function describing the helical system is

$$\psi(s + 2\pi a\cos\beta,\ at = 2\pi a\sin\beta) \equiv \psi(s,\ at = 0) \qquad \text{for all } s. \tag{3}$$

(iii) By definition, the pitch p of the helix is a translation along z accompanied by a 2π rotation in the θ-direction. This implies that $z \to z + p$, and $\theta \to \theta + 2\pi$, which in the helical system corresponds to a simple translation $s \to s + s_p$ along the s-direction with t unchanged. Here s_p is the length along the helix associated with one pitch, $s_p = p/\sin\beta$. The wave function under such a transformation can then change at most by a phase factor, $\exp(i\phi)$:

$$\psi(s + s_p, t) = \exp(i\phi)\psi(s, t) \qquad \text{for all } s, t. \tag{4}$$

It is thus natural to label the wave functions of the electrons in this system by the eigenvalues, M, of the operator P_S, the momentum operator along the helix. Equation (4) then leads to the result that M is a continuous eigenvalue. In addition we choose a second operator, $P_t \equiv (a^{-1}\sin\beta)\, L - \cos\beta P$, which commutes with P_S, and whose eigenvalues M' will provide us with a second quantum number to label the wave function of the electrons in the helical space. Thus we obtain a complete orthonormal set of helical-symmetry-adopted wave functions

$$\psi_{MM'}(s, t) = [\delta(\rho - a)/2\pi\sqrt{a\sin\beta}]\exp i(Ms + M't). \tag{5}$$

The δ-function in ρ represents the electrons as being localized to stay on the surface of the cylinder of radius a. A relation between M and M' exists following from the condition (3):

$$M' = (m - aM\cos\beta)/\sin\beta \qquad m = 0, \pm1, \pm2, \ldots. \tag{6}$$

The phase ϕ in equation (4) is Ms_p. Equation (5) may thus be rewritten in an equivalent form using (M, m) quantum numbers. To appreciate the significance of this representation we here state the complete set of orthonormal cylindrical wave functions is the eigenstates k, l respectively of the translation operator P and the rotation operator L, which commutes with it. Here k is continuous, and l is discrete, taking values $0, \pm1, \pm2, \ldots$. Explicitly these wave functions are

$$\psi_{kl}(z, \theta) = [\delta(\rho - a)/2\pi\sqrt{a}]\exp i(kz + l\theta). \tag{7}$$

The right-hand side of equation (2) may also be identified as the effective generator of translation parallel to the z-axis of the helix, $P_{\text{eff}} \equiv (\sin\beta)^{-1}P_S$. The eigenvalues of P_{eff} are then $K = k + 2\pi l/p$. When the pitch $p = \infty$, i.e., $\beta = \pi/2$, the helical states in equation (5) go over to the cylindrical states given by equation (7) and $l = m$.

The free one-electron energies associated with the cylindrical and helical symmetries are shown in figure 2 for fixed β, p. they are the familiar free electron parabolic energy bands associated with the cylindrical and helical symmetries. By invoking the periodicity along the helix, we obtain a one-dimensional Brillouin zone (BZ) feature in the M-direction, and the bands then will be folded back into the first BZ. These are the 'empty helix' bands, which become altered further when the actual atomic potential effects are included in the computation of the energy bands leading to the interesting features of the helical systems mentioned in the introductory paragraph. From figure 2 we see that the helical symmetry changes the nature of the free electron states given by $E_{Mm} = (2\mu)^{-1}[(M - m\cos\beta/a)^2(\sin\beta)^{-2} + m^2/a^2]$ from that of cylindrical symmetry in several ways. For example, there is no degeneracy between the $+m$ and $-m$ states when $m \neq 0$, and two minima in E_{Mm} occur at $\pm m\cos\beta/a$. In the presence of a constant

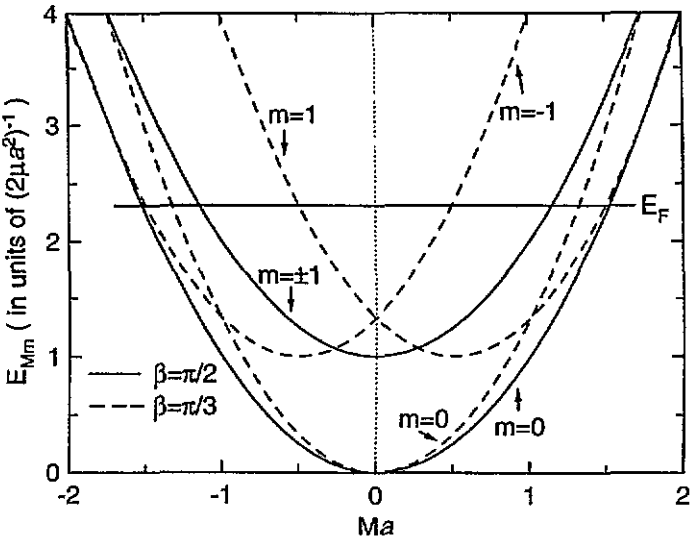

Figure 2. The free electron energy dispersion relations for $m = 0, \pm 1$ for representative pitch angle β.

magnetic field along the axis of the cylinder, this difference becomes even more significant as shown in [9].

We now show how to incorporate a periodic arrangement of atoms located on the surface of a cylinder in a helical motif in a description of its one-electron states using our helical waves. There may be only a single helical arrangement as in the case of some polymer chains [14], and as in figure 1(b), ABC'D' has no atoms in the interior of the parallelogram. Or, there may be several helices running along the surface of the cylinder, in which case the parallelogram ABC'D' will contain inequivalent lines parallel to AC' depicting the atomic arrangements on them. These atomic arrangements may or may not be periodic along the z-axis of the cylinder. In general, a periodicity $s_c = g's_p$ is possible where g' need not be an integer, and s_c is the repeat distance of the atomic pattern along the s-direction. We then define a unit rectangular cell in (s, at) space with dimensions s_c and $2\pi a \sin\beta$.

The helical Bloch functions with quantum numbers M and M' signifying the eigenvalues of P_S and P_t for a general multi-helix periodic system are given by

$$\Psi_{MM'}(s, t) = \sum_n \sum_{j(n)} \sum_A C_{A,n,j(n)} \Psi_{MM'}(s_{j(n)}, t_n) \varphi_A(s - s_{j(n)}, t - t_n). \quad (8)$$

Here $\varphi_A(s-s_{j(n)}, t-t_n)$ is the Ath atomic orbital associated with atoms situated at $(s_{j(n)}, at_n)$ in the unit cell, and $C_{A,n,j(n)}$ are the coefficients of the expansion. The sum over $j(n)$ is over the J_n atoms along the nth helix of length s_c, and the sum over n is over the different helices in the unit cell. It is often possible to have further rotational symmetry among the atoms in different spirals in the unit cell, as in the graphitic tubules. The wave functions in equation (8) have the required symmetries of the tubule and should satisfy the periodic conditions, equation (3) and

$$\Psi_{MM'}(s + s_c, t) = \Psi_{MM'}(s, t) \exp iMs_c. \quad (9)$$

Equation (3) leads to the same relation between M and M' as given in equation (6), while equation (9) defines the one-dimensional BZ in M: $(-\pi/s_c, \pi/s_c)$. This completes our description of helical Bloch band theory.

This theory is applicable for general helical systems that do not form two-dimensional Bravais lattice systems when unrolled into a flat $[z', a\theta]$ plane. We will now relate the parameters used here for the helical system to those generated by rolling a periodic graphitic motif into a cylinder described in the current literature (see the review in [8]). This provides us with a comparison of our approach with those in the literature. We shall henceforth focus attention on the graphitic tubules.

Following [7, 8] let $\boldsymbol{R}_1$ and $\boldsymbol{R}_2$ be two primitive lattice vectors of a sheet of the honeycomb lattice. A general tubule labelled by a pair of integers $\{n_1, n_2\}$ is obtained from a lattice vector $\boldsymbol{R} = n_1\boldsymbol{R}_1 + n_2\boldsymbol{R}_2$ by rolling the sheet with $\boldsymbol{R}$ as the base around the z-axis perpendicular to $\boldsymbol{R}$, into a cylinder of radius $a = |\boldsymbol{R}|/2\pi$. The period along the z-direction on this cylinder is obtained by finding the smallest lattice vector $\boldsymbol{S} = s_1\boldsymbol{S}_1 + s_2\boldsymbol{S}_2$ (s_1 and s_2 are integers) such that the vector $\boldsymbol{c} = (\boldsymbol{S} - \boldsymbol{R})$ is perpendicular to $\boldsymbol{R}$. This leads to the condition

$$(s_1 - n_1)(2n_1 + n_2) + (s_2 - n_2)(2n_2 + n_1) = 0. \tag{10}$$

The magnitude of the vector c gives us the lattice period along the tubule axis:

$$c = \left(|s_1 - n_1|/|2n_2 + n_1|\right)\left(n_1^2 + n_2^2 + n_1n_2\right)^{1/2}\sqrt{3}|\boldsymbol{R}_1|. \tag{11}$$

The spiral motif on the cylinder, on the other hand, is obtained by finding a vector $\boldsymbol{H} = h_1\boldsymbol{R}_1 + h_2\boldsymbol{R}_2$ that is a lattice vector along the spiral direction. It is convenient to choose $\boldsymbol{H}$ as the smallest lattice vector along the direction connecting one atom with its nearest neighbour. In our formulation the pitch angle, β, is thus given in terms of $\boldsymbol{H}$ by

$$\tan\beta = |\boldsymbol{H} \times \boldsymbol{R}|/(\boldsymbol{H} \cdot \boldsymbol{R}) \qquad \text{with } 0 < \beta \leqslant \pi/2 \tag{12}$$

and the pitch p is given by

$$p = |\boldsymbol{R}| \tan\beta. \tag{13}$$

We then observe that $c/p = g$ is in general rational, but when it is an integer it gives the number of turns of the spiral in the periodic unit cell on the cylinder. Also the area of the unit cell is an integral multiple of the area $\Delta = |\boldsymbol{R}_1 \times \boldsymbol{R}_2|$ of the unit cell of the underlying two-dimensional sheet, so that we have the relation

$$|\boldsymbol{S} \times \boldsymbol{R}| = \left[\left(2|s_1 - n_1|\right)/\left(2n_2 + n_1\right)\right]\left(n_1^2 + n_2^2 + n_1n_2\right)\Delta. \tag{14}$$

Thus $\boldsymbol{S}$ is determined by the period along the z-direction, and $\boldsymbol{H}$ is determined by the helical path chosen to describe the helical symmetry.

All tubules constructed in this way therefore possess helical structures. There are two special types of tubule of interest, namely the serpentine, $\{n, n\}$, and the sawtooth, $\{n, 0\}$, both of which have reflection planes and are thus achiral, whereas all others are chiral. Figure 3 exhibits special cases of these two types and figure 4 represents another tubule {6, 3}, which is an example of a chiral tubule. In the serpentine case, we choose $\boldsymbol{H} = -\boldsymbol{R}_1 + 2\boldsymbol{R}_2$, and in all other cases we choose $\boldsymbol{H} = \boldsymbol{R}_1 + \boldsymbol{R}_2$. We thus have the following.

(i) *Serpentine* $\{n, n\}$:

$$\beta\{n, n\} = \pi/3 \qquad c\{n, n\} = |s_1 - n||\boldsymbol{R}_1| \qquad p\{n, n\} = 3n|\boldsymbol{R}_1| \tag{15}$$

so that $g\{n, n\} = |s_1 - n|/3n$. From equation (1) the smallest S for this case has $|s_1 - n| = 1$, and thus $g\{n, n\} = 1/3n$. As shown in figure 3(a), for $\{1, 1\}$, $s_1 = 2$, $s_2 = 0$, and g is shown to be $\frac{1}{3}$.

(ii) *Sawtooth* $\{n, 0\}$:

$$\beta\{n, 0\} = \pi/6 \qquad c\{n, 0\} = \sqrt{3}|\boldsymbol{R}_1||s_1 - n| \qquad p\{n, 0\} = n|\boldsymbol{R}_1|/\sqrt{3} \tag{16}$$

so that $g\{n, 0\} = 3|s_1 - n|/n$. The case $\{3, 0\}$ with $s_1 = s_2 = 2$, as shown in figure 3(b), satisfies the conditions in equation (16), and thus $g = 1$.

(iii) $\{6, 3\}$ *tubule*

$$\beta\{6, 3\} = \tan^{-1}(\sqrt{3}/9) \qquad c\{6, 3\} = (\sqrt{21}|s_1 - 6|/4)|\boldsymbol{R}_1| \qquad p\{6, 3\} = \sqrt{\tfrac{7}{3}}|\boldsymbol{R}_1|. \tag{17}$$

Since from equation (10) $s_1 = 2$, $s_2 = 8$, we have $g\{6, 3\} = 3$ from equation (17). This tubule is displayed in figure 4.

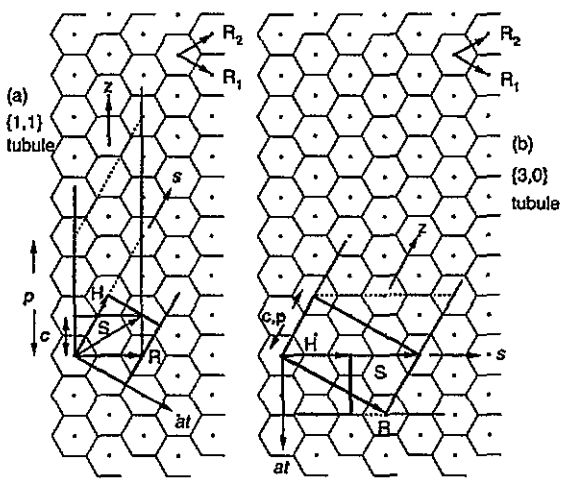

Figure 3. Two-dimensional graphite sheets with six atoms at the corners of each hexagon. The graphitic tubules are constructed by rolling the rectangular strips with base $\boldsymbol{R}$ around the tubule axis z for (a) the $\{1, 1\}$ serpentine tubule and (b) the $\{3, 0\}$ sawtooth tubule. $\boldsymbol{H}$ is in the direction of the spirals. Dotted lines and the line along the $\boldsymbol{H}$ direction form a continuous spiral in each tubule. The rectangles in heavy lines are the periodic cells in $[z', a\theta]$ space and in (s, at) space.

The energy bands for the serpentine and the sawtooth types of tubule have been obtained in [10] and [11] by folding the two-dimensional bands associated with the graphite sheet along the k_x and k_y directions respectively. For a general graphitic tubule $\{n_1, n_2 \neq n_1 \neq 0\}$, White *et al* [6,7] obtain the band structure by effectively transforming the two-dimensional graphite bands in the (s, at) space of the tubule in terms of the $[z', a\theta]$ representation

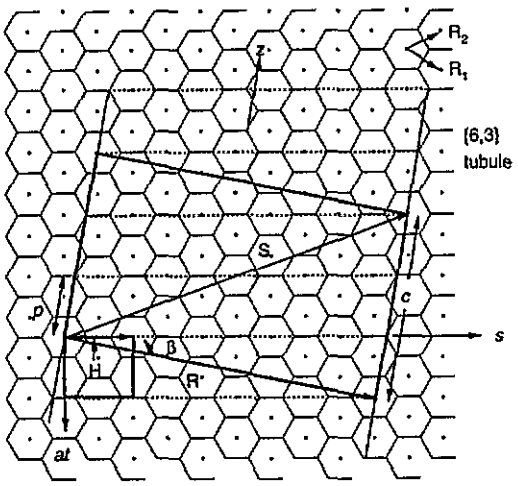

Figure 4. The construction of a {6, 3} graphitic tubule from the two-dimensional graphite sheet. Dotted lines form a continuous spiral after rolling the sheet into a cylinder. Three twists of a given spiral create a periodicity in the z-direction. The two rectangles bounded by heavy lines are the respective periodic cells in $[z', a\theta]$ space and in (s, at) space.

and introduce two integers to take into account the folding of the bands in the direction perpendicular to the cylinder axis. We will now show that our helical Bloch formulation can be used directly in (s, at) space with the folding of the bands following straightforwardly in the cases considered. An important advantage of using our approach is that the size of the unit cell is in general reduced drastically from that in the $[z', a\theta]$ representation.

Consider the {6, 3} tubule, which is depicted in figure 4. It consists of 84 atoms in the unit cell of $[z', a\theta]$ space. The period along the z-direction is $3p$. However, in (s, at) space this tubule consists of only six atoms in the unit cell. Here $g' = (s_c/s_p) = \frac{3}{14}$, $s_c = |R_1|/\sqrt{3}$. This follows from equations (12) and (13). Another interesting feature in this description is that the three types of tubule, {6, 3}, {1, 1}, and {3, 0} all have the same unit cell in (s, at) space although they appear to be entirely different in $[z', a\theta]$ space as shown in figures 3 and 4.

To evaluate the band structure of the {6, 3} tubule in our scheme, we first construct the Bloch function given by equation (8) with the sum running over the six basis atoms of the unit cell with one-dimensional translation symmetry along the s-axis. The coordinates of the six atoms in (s, at) space are $(d, 0)$, $(2d, 0)$, $(d/2, \sqrt{3}d/2)$, $(3d/2, \sqrt{3}d/2)$, $(d, \sqrt{3}d)$, $(2d, \sqrt{3}d)$, with d as the nearest-neighbour distance. Assuming that each atom is interacting with its three nearest neighbours and that only π bonds are taken into consideration, ignoring the small changes due to the curvature of the tubule surface, we finally obtain a 6×6 Hamiltonian matrix for determining the band structure. The neighbours outside the unit cell are mapped back to the equivalent atoms inside the unit cell by translation symmetry. Thus all the important interactions between atoms on the spirals are taken into account. We thus obtain the energy bands $E_{MM'}$ for the tubule by solving the equation

$$y^6 - 9y^4 + 12(2 - \cos^2\alpha - \cos\alpha\cos\gamma)y^2 - 4(4 + \cos^2\gamma - 3\cos^2\alpha - 6\cos\alpha\cos\gamma + 4\cos^3\alpha\cos\gamma) = 0. \tag{18}$$

Here $y = E_{MM'} - E_0$, E_0 is the atomic orbital energy, $\alpha = 3Md/2$, and $\gamma = 3\sqrt{3}M'd/(2a)$.

Corresponding to the given integer value of m, there is a set of six one-dimensional subbands given by the solutions of equation (18). Thus we obtain the energy bands of the tubule as being composed of many one-dimensional subbands. This corresponds to the creation of many one-dimensional bands by folding the rectangular graphitic sheet into a cylinder as in [10]. Because of the small number of atoms in the unit cell this problem reduces to solving equation (18).

Two of the solutions of equation (18) are easily obtained:

$$y^2 = 1 + 4\cos\frac{\gamma}{3}\cos\alpha + 2\cos\frac{2\gamma}{3} = 3 + 2\cos\frac{(3M + \sqrt{3}M'/a)d}{2}$$
$$+ 2\cos\frac{(3M - \sqrt{3}M'/a)d}{2} + 2\cos(\sqrt{3}M'd/a). \tag{19}$$

This reduces, after a transformation to $[z', a\theta]$ space, to the result obtained in [7] with no folding condition imposed. This transformation is found from equations (5) and (7) to be

$$M = (l/a)\cos\beta + k\sin\beta \qquad M' = l\sin\beta - ak\cos\beta. \tag{20}$$

For the tubule $\{n_1, n_2 \neq n_1\}$, with $\boldsymbol{H} = \boldsymbol{R}_1 + \boldsymbol{R}_2$, β is found to be

$$\tan\beta = (n_1 - n_2)/\sqrt{3}(n_1 + n_2) \tag{21}$$

from equation (12). Identifying k, l with the quantities employed in [7], we obtain their expression for the band structure from equation (19). The other four solutions of equation (18) correspond to the results obtained by folding the solutions of equation (19) twice in the $a\theta$ direction. As pointed out above, the structure of the solutions for the other two tubules, {1, 1} and {3, 0}, are formally the same as above and the differences lie in the appropriate pitch angle β, and in the projected periodicity s_c along the respective spirals. These give rise to different sizes of the reduced zone and hence to the different times of further folding of the energy bands in the s-direction. This is reminiscent of taking the free electron parabolic band and then obtaining the appropriate zone foldings corresponding to different crystal structures. We have thus shown a great advantage in the use of helical Bloch functions constructed here in obtaining the band structures of a variety of spiral structures once an equation of the type of (18) is set up. We may point out that lattice vibrational frequencies and other similar properties can all be calculated by suitably adopting this technique.

We will now obtain a criterion for the existence of a narrow gap in a graphitic tubule in our formalism. Since we have neglected the curvature effects due to the cylindrical structure, the bonding and the antibonding π bands are degenerate at the corner points of the first BZ of the two-dimensional graphitic sheet. In our helical reciprocal space this corresponds to the special values $M = \pi/s_c$, $M' = a\pi/(s_c\sqrt{3})$. After using the relationship between M and M' in equation (6), we obtain the following condition for the tubule to have a narrow band gap:

$$(\pi a/s_c)(\cos\beta + \sin\beta/\sqrt{3}) = m \tag{22}$$

m being any integer. This is an alternate but equivalent result to that obtained in [6], [10] and [11].

In addition to the reduced size of the unit cell, the assignment of the atomic positions in the unit cell and the separation of the summation in equation (8) into each individual spiral

make possible a physical determination of the mutual interaction between the spirals on the same cylinder in discussing both the electronic and vibrational properties of this system.

Experimentally, one often finds concentric tubules, not isolated single tubules [2]. One often neglects the inter-tubule hopping of electrons in theoretical studies in view of the fairly large distance between the tubules and the lack of strong bonding in the radial direction. However, the long-range two-particle Coulomb interactions have to be considered. In [9], we have considered the effects of the helical structures on the two-particle intra- and inter-tubule Coulomb matrix elements and contrasted with the cylindrical (non-helical) case. These exhibit a one-dimensional behaviour for $a_s M \ll 1$ (logarithmic for $m = 0$ and finite for $m \neq 0$), and two-dimensional features for $a_s M \gg 1$. Here a_s is the radius of the innermost cylinder. The inter-tubule interactions resemble the inter-layer interactions in a layered system. Also, the inter-tubule interactions are found to be weaker than the intra-tubule interactions as expected.

In conclusion, we have here constructed helical Bloch wave functions for studying the electronic structure of tubules possessing helical symmetry. We have demonstrated how this method is complementary to the existing methods in the literature. This approach is based directly on the helical properties in contrast to the approaches in the literature where the two-dimensional Bravais lattice is rolled into a cylinder. Therefore it should be suitable in cases where only helical symmetry exists and that cannot be obtained by rolling a structure that does not form a periodic two-dimensional lattice into a cylinder.

Acknowledgments

Dr Carter White introduced us to the interesting tubule systems and provided us with his papers before publication and also discussed various aspects of the problem. It is a pleasure to thank him for all his guidance and help. We thank Dr A Saxena for sending us a copy of his preprint [5]. This work was supported in part by the Office of Naval Research.

References

[1] Iijima S 1991 *Nature* **354** 56
[2] Ebbesen T W and Ajayan P M 1992 *Nature* **358** 220
[3] Wang L, Davids P S, Saxena A and Bishop A R 1992 *Phys. Rev.* B **46** 7175
[4] Lin M F and Shung K W 1993 *Phys. Rev.* B **47** 6617; 1993 *Phys. Rev.* B **48** 5567
[5] Davids P S, Wang L, Saxena A and Bishop A R 1994 *Phys. Rev.* B **49** 5682
[6] Mintmire J W, Dunlap B I and White C T 1992 *Phys. Rev. Lett.* **68** 631
[7] White C T, Robertson D H and Mintmire J W 1993 *Phys. Rev.* B **47** 5485
[8] White C T, Mintmire J W, Mowrey R C, Brenner D W, Robertson D H, Harrison J A and Dunlap B I 1993 *Buckminsterfullerenes* ed W E Billups and M A Ciufolini (New York: VCH) p 125
[9] Lin-Chung P J and Rajagopal A K 1994 *Local Order In Condensed Matter* ed P Jena and S D Mahanti (New York: Nova); 1994 *Phys. Rev.* B **49** 8454
[10] Saito R, Fujita M, Dresselhaus G and Dresselhaus M S 1992 *Phys. Rev.* B **46** 1804
[11] Hamada N, Sawada S I and Oshiyama A 1992 *Phys. Rev. Lett.* **68** 1579
[12] Ajiki H and Ando T 1993 *J. Phys. Soc. Japan* **62** 1255
[13] Yi J Y and Bernholc J 1993 *Phys. Rev.* B **47** 1708
[14] Mintmire J W 1991 *Density Functional Methods in Chemistry* ed J K Labonowski and J W Andzelm (New York: Springer) p 125